Self-assembled ordered polymer nanocomposites directed by attractive particles

C. D. Knorowski,[1,2] J. A. Anderson,[1] and A. Travesset[1,a)]
[1]*Ames Laboratory and Department of Physics and Astronomy, Iowa State University, Ames, Iowa 50011, USA*
[2]*Department of Physics, Virginia Tech, Blacksburg, Virginia 24061, USA*

(Received 8 February 2008; accepted 18 March 2008; published online 24 April 2008)

We theoretically investigate general conditions under which an inorganic phase can direct the self-assembly of an ordered polymer nanocomposite. For this purpose, we consider a solution of triblock copolymers forming a hexagonal phase of micelles and investigate the effect of adding attractive particles. We show that if the triblock is functionalized at its ends by attaching groups with specific affinity for the particles, thus effectively becoming a pentablock, the particles direct the self-assembly of the system into phases where both the polymers and the particles exhibit mesoscopic order. Different lamellar and gyroid phases (both with $Ia\bar{3}d$ and $I4_132$ space symmetries) are presented in detail. Our results show that functionalization is a very powerful route for directing self-assembly of polymer nanocomposites. We briefly discuss the connections with recent theoretical and experimental results in diblock melts with nanoparticles as well as for problems where polymers are used to template the growth of an inorganic phase in solution.
© *2008 American Institute of Physics*. [DOI: 10.1063/1.2907744]

The fascinatingly rich phase diagram of block copolymer solutions and melts[1,2] is vastly expanded when combined with inorganic components such as nanoparticles. A very exciting possibility is that inorganic particles in solution could direct the particular mesoscopic order of the polymer/inorganic composite. These polymer nanocomposite crystals offer huge possibilities for new materials with exquisitely tuned optical, mechanical, or transport properties.[3]

Multiblock copolymers containing both hydrophilic and hydrophobic blocks are particularly suitable, as they generally aggregate into micelles whose geometry and structure can be tightly controlled by varying the hydrophobic/hydrophilic ratio or by external conditions such as temperature or *p*H. A pertinent example is provided by Pluronic or poloxamer polymers, short symmetric triblocks (*ABA*) where the *B*-block is polypropylene oxide and the *A*-block is polyethylene oxide. Pluronics are particularly versatile, as they exhibit a myriad of phases over narrow temperature and concentration regions.[1]

In this paper, we investigate general conditions under which an inorganic phase can direct the self-assembly of an ordered polymer nanocomposite. Because of our ongoing interest in Pluronics, we will consider a generic *ABA* triblock coexisting with inorganic particles, which herein will be referred to as monomers. Physically, monomers are single or small clusters of inorganic molecules subnanometer in size. We assume that the inorganic particles tend to crystallize, so monomers will attract each other with a characteristic energy ε_N (see Fig. 1). In the absence of any specific interaction between polymer and monomers, ordered nanocomposites can only occur by templating, where the polymeric phase is able to coerce monomer aggregation and direct it toward the regions occupied by the solvent. In this paper, we consider functionalized polymers, where both end blocks of the triblock are functionalized by covalently attaching a group with high affinity for the monomers (see Fig. 1). In this way, the end groups provide multiple centers for nucleating the aggregation of the inorganic phase. Functionalization is modeled by introducing an energy scale ϵ_F, the energy gain for monomers to bind to the functionalized group. Experimentally, methods for functionalizing polymers are available, and there is a considerable repertoire of groups that can be attached, for example, to Pluronics.[4]

We model a generic Pluronic, such that the pure system forms a hexagonal phase. In this paper, we consider an $A_6B_7A_6$ polymer. The monomers are modeled as single beads (see Fig. 1). The interactions follow from Ref. 5. The solvent is considered implicitly and the nonbonded potentials are described according to

$$V(r) = 4\varepsilon_{IJ}\left[\left(\frac{\sigma}{r}\right)^{12} - \alpha_{IJ}\left(\frac{\sigma}{r}\right)^{6}\right]. \tag{1}$$

B beads are hydrophobic, while *A* beads are hydrophilic $\varepsilon_{AA}=\varepsilon_{BB}=\varepsilon_{AB}\equiv\varepsilon_P$ and $\alpha_{AA}=\alpha_{AB}=0$, $\alpha_{BB}=1$. Monomer-polymer interactions are described by $\alpha_{NN}=\alpha_{NA,B}=0$ and $\varepsilon_{NA}=\varepsilon_{NB}=\varepsilon_P$, while monomer-monomer interactions by $\varepsilon_N \equiv \varepsilon_{NN}$, which is a free parameter, and $\alpha_{NN}=1$. Functionalized polymers are described by the same parameters except for the two end beads, given by $\varepsilon_F \equiv \varepsilon_{AN}$ (see Fig. 1), the second free parameter of the model, and $\alpha_{AN}=1$.

All beads in our model have the same mass *m* and interaction range σ. Simulations are carried out with the LAMMPS simulations package.[6] A number N_{poly} of polymers are considered in a finite cube of length *L* (in units of σ) with peri-

a)Electronic mail: trvsst@ameslab.gov.

 © 2008 American Institute of Physics

Downloaded 14 May 2008 to 129.186.151.28. Redistribution subject to AIP license or copyright; see http://jcp.aip.org/jcp/copyright.jsp

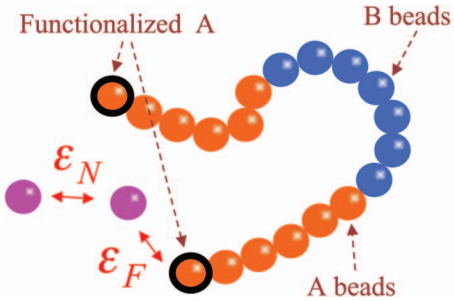

FIG. 1. (Color) Schematic representation of the system considered. An *ABA* triblock ($A=6,B=7$) functionalized polymer. The monomers are single beads that attract each other with characteristic energy ε_N, and with an energy ε_F to the functionalized *A* beads.

odic boundary conditions. The polymer packing fraction ϕ_P is related to L and N_{poly} by $\phi_P=\pi N_{\text{poly}}N_{\text{mon}}/6L^3$, where $N_{\text{mon}}=19$ is the number of beads per polymer. ε_P/k_BT is fixed at 0.8333.

All results were obtained with a polymer fraction $\phi_P=0.25$, where the $A_6B_7A_6$ polymer without monomers is found in a hexagonal phase. The monomer fraction was fixed at 5% (about two monomers per functionalized group). The simulation runs took between 2×10^6 and 3×10^6 steps, depending on the system size and the phase. In most cases, in order to ensure reproducibility, different initial configurations were tested. Additional technical details can be found in the Auxiliary Materials.[8] Ordered structures are analyzed by computing the static structure factor

$$S_{JJ}(\mathbf{q}) = C_J \sum_{k=1} \sum_{l=1} \langle e^{i\mathbf{q}(\mathbf{r}_k^J-\mathbf{r}_l^J)}\rangle, \tag{2}$$

where $J=A,B$, or N refer to hydrophilic, hydrophobic, or monomer beads. C_J is chosen so that $S_{JJ}(0)=1$.

Simulations spanning system sizes between $N_{\text{poly}}=400-3000$ were performed (see the auxiliary material for details). The most recurrent phases at various system sizes were considered thermodynamically stable. The phase diagram best summarizing all simulation results is shown in Fig. 2. Obviously, phase boundaries cannot be determined with precision.

We first discuss nonfunctionalized polymers ($\varepsilon_F/k_BT \ll 1$). For weakly attracting monomers ($\varepsilon_N/k_BT \ll 1$), thermal

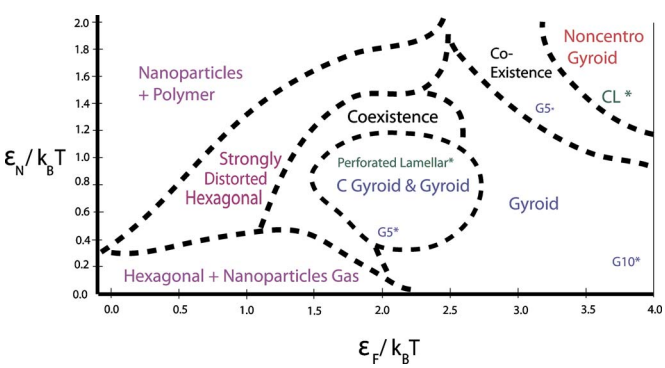

FIG. 2. (Color online) Phase Diagram as a function of monomer-monomer (ε_N) and monomer-functionalized end (ϵ_F) interaction for a concentration of 5% polymers at $k_BT/\epsilon_P=1.2$. Phases with asterisks are expected to have a narrow stability range or to be metastable.

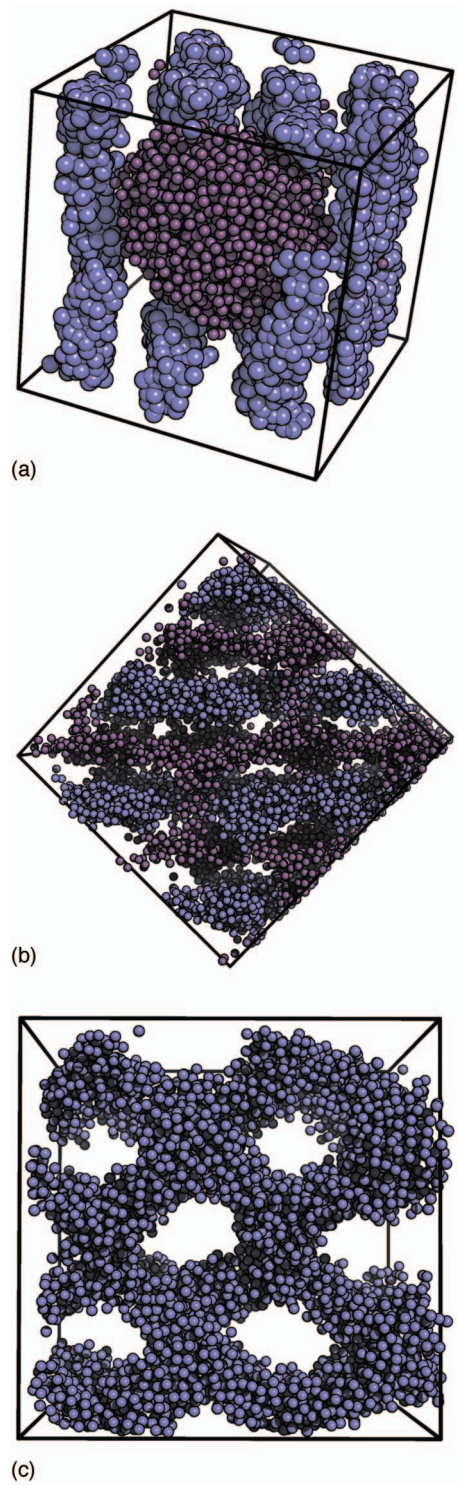

FIG. 3. (Color) (a) Snapshot of nonfunctionalized polymers and monomers, an example of a failed template. (b) Snapshot of the perforated lamellar nanocomposite. (c) Snapshot of the perforated lamellar without the monomers showing that the perforations form a hexagonal lattice. The *B* beads are blue and monomers purple. In all cases, the hydrophilic *A* beads are omitted for clarity. All snapshots are created with PYMOL [Ref. 7].

effects prevent monomer aggregation and the micelles remain in the hexagonal phase while the monomers are in a gas "nanoparticle gas" phase, freely diffusing within the solvent. As monomer attraction is increased $\varepsilon_N/k_BT\sim1$, monomers eventually aggregate into a spherical blob (fluid or crystalline), as shown in Fig. 3(a). The polymeric matrix is unable

Downloaded 14 May 2008 to 129.186.151.28. Redistribution subject to AIP license or copyright; see http://jcp.aip.org/jcp/copyright.jsp

to template as the monomers segregate from the polymer phase (nanoparticle+polymer in Fig. 2).

In the weakly functionalized case $\varepsilon_F/k_BT \lesssim 1$, monomers distort the polymeric matrix, which roughly maintains its hexagonal form. Interesting results occur for $\varepsilon_F/k_BT \gtrsim 2$; Here, ordered nanocomposites with lamellar and gyroid order (see Fig. 2) are organized at the expense of the original hexagonal phase.

A snapshot of a perforated lamellar phase, where the monomers are successfully ordered is shown in Fig. 3(b). The perforations form a two dimensional hexagonal lattice [see Fig. 3(c)]. Quite remarkably, the lamellar planes and the perforations are uniformly covered with monomers. The fact that the perforated lamellar phase was not found in all system sizes (see the auxiliary material) raises the possibility that it is metastable or that its stability domain is narrow.

Gyroids are the most prevalent phases. Representative snapshots are shown in Fig. 4 a typical structure factor confirming the gyroid structure is shown in Fig. 6(a). The monomers show interesting variations in their structure. In Fig. 4(b), it is shown that monomers exhibit an almost perfect two dimensional curved surface, which we denote as a carpeted (C) gyroid, while in most other cases, a structure like the one in Fig. 4(c) is found. The analysis of the structure factor Fig. 6(a) shows that both the monomers and the hydrophobic blocks conform to the $Ia\bar{3}d$ symmetry, thus providing clear evidence for mesoscopic order. Occasionally, gyroids with structure factors showing peaks not allowed by the $Ia\bar{3}d$ symmetry, such as $\sqrt{5}$ and $\sqrt{10}$, indicated as G^5 and G^{10} in Fig. 2 are found, suggesting distortions due to a lattice constant incommensurate with the simulation box size, a point that will be elaborated elsewhere.

For strongly attracting monomers and $\varepsilon_F/k_BT \gtrsim 3$, the unit cell of the gyroid becomes noncentrosymmetric, thus reducing the space group symmetry from $Ia\bar{3}d$ to $I4_132$. In Fig. 5(b), a snapshot of the noncentrosymmetric gyroid is shown, where it is quite apparent that the simulation box contains two unit cells per linear dimension (eight in total). An analysis of the structure factor, Fig. 6(b), confirms the $I4_132$ symmetry and the size of the unit cell. The monomers are arranged according to the $I4_132$ symmetry [see Fig. 5(c)for a snapshot].

In the region where noncentrosymmetric gyroids are found, a new checkerboard lamellar (CL) phase was observed in some system sizes. The CL phase consists of lamellar planes, where each lamellar plane contains patches of monomers and polymers, as shown in Fig. 5(a). This phase, however, was not consistently found in all system sizes and it is possibly metastable.

The structure factor for the lamellar phases were also computed and showed the expected peaks (results not shown). Regions of the phase diagram that did not settle into definite phases are indicated as mixed regions.

A first, but important result in this paper is that in the absence of specific interactions between the polymer and the inorganic particles, no mesoscopic order is imposed into the monomers. Contrary to what happens in melts,[9] the polymeric matrix in solution is not rigid enough to direct the growth of the inorganic phase [see Fig. 3(a)].

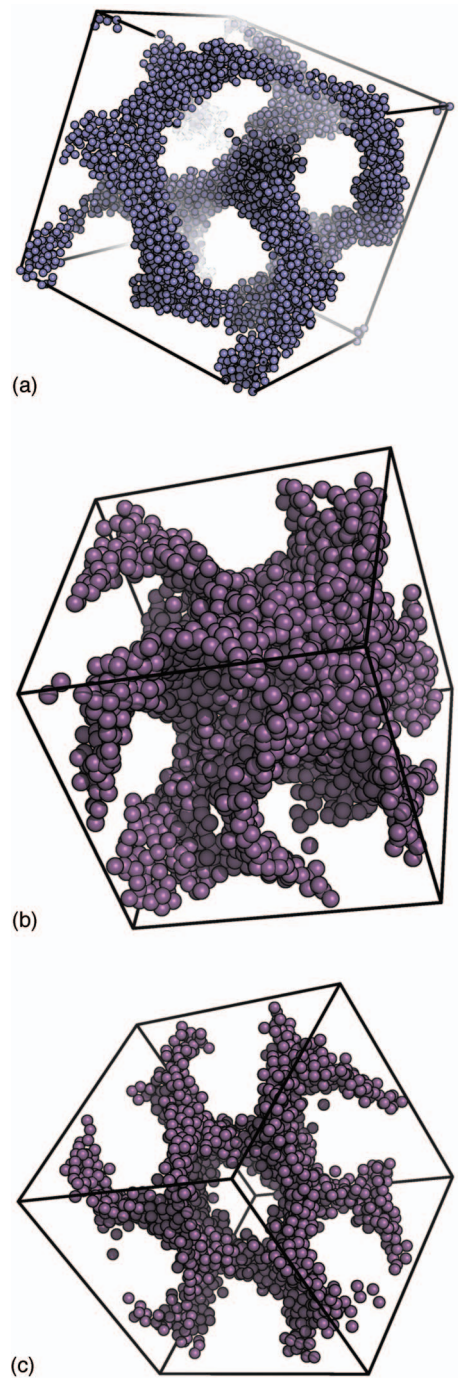

FIG. 4. (Color) (a) Snapshot of a gyroid (space group $Ia\bar{3}d$) where only B beads are displayed. (b) Example of the monomers in a carpeted gyroid. (c) Monomers in a regular gyroid. In all cases, monomers are ordered with the $Ia\bar{3}d$ space group.

Functionalization does provide successful ordered mesostructures. In Ref. 10 it has been shown that an AB diblock melt with added "Janus" nanoparticles (with affinity for both A and B blocks) destabilize a lamellar phase into bicontinuous structures (such as the gyroid). Following Ref. 11, the bicontinous phases are explained by the reduction in surface tension induced by the adsorbed nanoparticles at the AB interface, thus reducing polymer stretching. Our system starts from cylindrical micelles, so the effect of the attractive

Downloaded 14 May 2008 to 129.186.151.28. Redistribution subject to AIP license or copyright; see http://jcp.aip.org/jcp/copyright.jsp

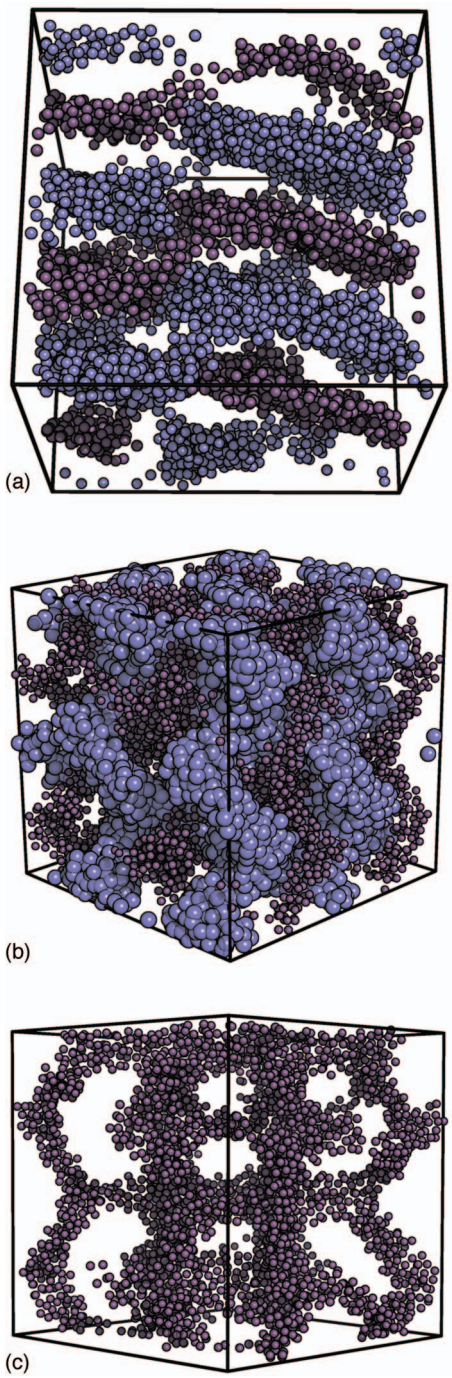

FIG. 5. (Color) (a) Snapshot of the checkerboard lamellar phase. (b) Snapshot of the non-centrosymmetric gyroid (space group $I4_132$). (c) Snapshot of the distribution of the monomers in the noncentrosymmetric gyroid (also ordered with the $I4_132$ space group).

monomers is to pull the end polymer blocks to the outside of the micelle corona, considerably stretching the hydrophilic blocks.[2] In general, the role of the attractive particles is to provide a "neutral surface" with negligible surface tension, leading to the minimal surfaces observed in the simulations (see Ref. 12 for some experimental evidence).

A different mechanism for stabilization of gyroid phases by nanoparticles has been described recently[13] in diblock melts, where the nanoparticles fill the gaps within gyroid nodes to reduce packing frustration. In the $\varepsilon_F/k_BT \gg 1$ limit, the functionalized polymers may bind several nanoparticles,

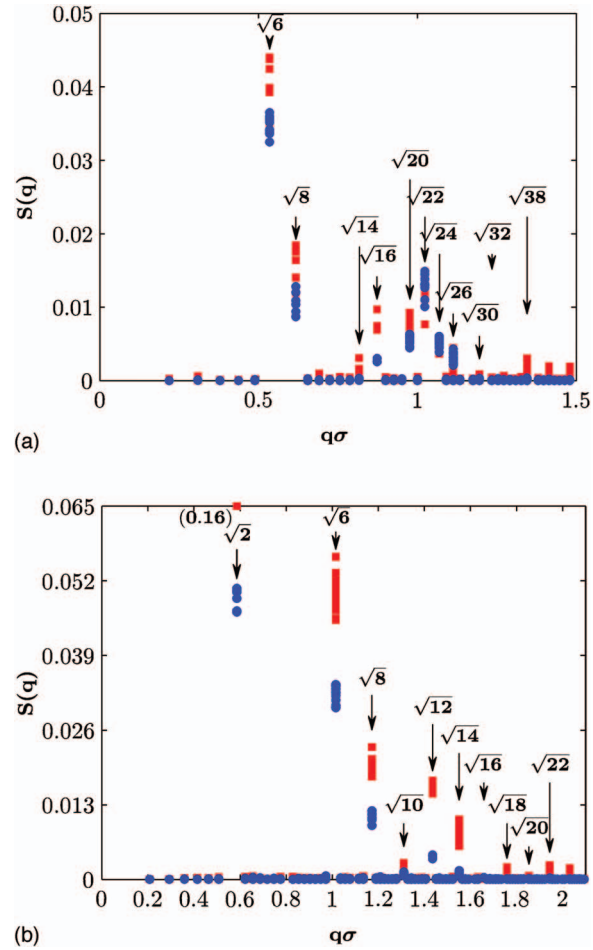

FIG. 6. (Color) (a) Structure factor of the gyroid ($N_{poly}=600$, $\varepsilon_F/k_BT=2.5$, $\varepsilon_N/k_BT=1.0$) with $Ia\bar{3}d$ space group with the expected location of the peaks. (b) Structure factor of the gyroid (700, 3.9, 1.8) with $I4_132$ space group. The structure factor for monomer beads is indicated by red squares while the one for the B beads is shown with blue circles.

thus resembling tethered polymers for $\varepsilon_N/k_BT \ll 1$, which also exhibit gyroid phases.[14] Our results suggest that tethered polymers with added hydrophobic blocks might enhance the range of stability of the gyroid phase. We should mention the relevance of our results to recent experiments with Pluronic and functionalized Pluronics[15] to template the growth of inorganic phases such as calcium phosphate or carbonate(see Auxiliary Materials[8] also).

In summary, the new conceptual insight in this paper is that polymer functionalization provides a robust strategy in which an inorganic phase directs the self-assembly of ordered polymer nanocomposite phases in solution. Further experimental and theoretical studies will provide a more detailed understanding.

We thank E. W. Cochran for many insightful comments on the manuscript and C. D. Santangelo for discussions. C. K. acknowledges support from the Ames lab SULI internship. This work is supported by DOE-BES through the Ames lab under Contract No. DE-AC02-07CH11358 and partially supported by the NSF Grant DMR-0426597.

[1] *Amphiphilic Block Copolymers: Self-Assembly and Applications* edited by P. Alexandridis and B. Lindman (Elsevier Science, Amsterdam, 2000).

Downloaded 14 May 2008 to 129.186.151.28. Redistribution subject to AIP license or copyright; see http://jcp.aip.org/jcp/copyright.jsp

[2] M. Matsen, J. Phys.: Condens. Matter **14**, R21 (2002).
[3] M. R. Bockstaller, R. A. Mickiewicz, and E. L. Thomas, Adv. Mater. (Weinheim, Ger.) **17**, 1331 (2005).
[4] B. Anderson, S. Cox, P. Bloom, V. Sheares, and S. Mallapragada, Macromolecules **36**, 1670 (2003).
[5] J. Anderson and A. Travesset, Macromolecules **39**, 5143 (2006).
[6] S. Plimpton, J. Comput. Phys. **117**, 1 (1995).
[7] W. L. DeLano, The PyMOL Molecular graphics system, San Carlos, CA, 2002 (http://www.pymol.org).
[8] See EPAPS Document No. E-JCPSA6-128-024817 for supplemental material regarding simulation and experimental details. For more information on EPAPS, see http://www.aip.org/pubservs/epaps.html.
[9] R. B. Thompson, V. Ginzburg, M. Matsen, and A. Balazs, Macromolecules **35**, 1060 (2002).
[10] B. J. Kim, G. H. Fredrickson, C. J. Hawker, and E. J. Kramer, Langmuir **23**, 7804 (2007).
[11] V. Pryamitsin and V. Ganesan, Macromolecules **39**, 8499 (2006).
[12] C. Lo, B. Lee, V. Pol, N. Dietz Rago, S. Seifert, R. Winans, and P. Thiyagarajan, Macromolecules **40**, 8302 (2007).
[13] F. Martinez-Veracoeachea and F. Escobedo, Macromolecules **38**, 8522 (2005); , J. Chem. Phys. **125**, 104907 (2006).
[14] C. Iacovella *et al.*, Phys. Rev. E **75**, 040801(R) (2007).
[15] D. Enlow, A. Rawal, M. Kanapathipillai, K. Schmidt-Rohr, and S. Mallapragada, J. Mater. Chem. **16**, 1570 (2007).

Downloaded 14 May 2008 to 129.186.151.28. Redistribution subject to AIP license or copyright; see http://jcp.aip.org/jcp/copyright.jsp